

Amplitude Control of Chemical Waves in Catalytic Membranes. Asymmetric Wave Propagation between Zones Loaded with Different Catalyst Concentrations

András Volford,[†] Zoltán Noszticzius,^{*,†} Valentin Krinsky,[‡] Christophe Dupont,[‡] Attila Lázár, and Horst-Dieter Försterling[§]

Center for Complex and Nonlinear Systems and the Department of Chemical Physics, Technical University of Budapest, H-1521 Budapest, Hungary, Institut Non Lineaire de Nice, UMR 129 CNRS-UNSA, 06560 Valbonne, France, and Fachbereich Physikalische Chemie, Philipps Universität Marburg, D-35032 Marburg/Lahn, Germany

Received: June 2, 1998

Chemical waves of the Belousov–Zhabotinsky type are studied applying bathoferroin catalyst fixed on a polysulfone membrane. A new method is developed to create contacting high- (H) and low-amplitude (L) regions for chemical waves. The amplitude is high in zones (H) loaded with high catalyst concentrations, and it is low in zones (L) loaded with low catalyst concentrations. An asymmetric wave propagation is found: waves coming from region H can initiate waves in region L across the HL boundary with a higher frequency than vice versa. The ratio of the cross-recovery times $R(L \rightarrow H)$ and $R(H \rightarrow L)$ is 1.7 in the experiments reported here. To measure this ratio, rotating chemical waves were applied. The waves propagate in two concentric annular zones—the inner zone with low and the outer with high catalyst concentration—and the HL boundary forms a circle. It was found that in such a reactor complex wave patterns (so-called chemical pinwheels) can rotate nearly independently in the H and L zones, interacting only weakly across the HL boundary.

Introduction

The experimental and theoretical investigation of traveling waves in excitable chemical¹ and biological² systems is one of the most active research areas in the field of nonlinear dynamics. The majority of the chemical wave experiments are made with the Belousov–Zhabotinsky (BZ) reaction since a first report by Zaikin and Zhabotinsky.³ In the beginning these experiments were performed in closed reactors (Petri dishes), applying a uniform liquid medium.^{4,5} Some of the early experiments applied silica gel or membrane filter⁶ to block the convection of the free liquid. Later on, more sophisticated open reactors appeared where the reaction was embedded in different hydrogels^{7–9} or its catalyst was fixed to various polymer membranes.^{10–13} Even these advanced studies applied an excitable medium, which was mostly homogeneous. Nevertheless, as the interest in nonlinear dynamics was shifting toward biological and more complex chemical systems, investigations on chemical waves propagating in nonuniform media continued to appear.^{14–23} Most recently²⁴ Agladze, Aliev, Yamaguchi, and Yoshikawa were able to construct a so-called “chemical diode” where propagation of chemical waves is unidirectional due to an asymmetrical geometry of the construction. In their diode, two square-shaped pieces of microporous Vycor Corning glass plates are applied. The two pieces are loaded with the same level of the BZ catalyst, but their geometrical arrangement is asymmetric. A planar (P) edge of one Vycor square faces with the corner (C) of the other square, separated by a thin gap of catalyst-free BZ solution. In the case of appropriate gap size

and chemistry, chemical waves are able to propagate from P to C but not in the reverse direction. This P-C diode with a gap has some similarity with a vacuum tube diode. In that device, the electrodes are separated by vacuum and the asymmetry is due to a hot cathode which emits many more electrons into the vacuum than the cold anode. Modern solid state electronics also applies diodes, but the working principle of a semiconductor diode is different. In that device the asymmetry is caused by the different dopants applied to create *p* and *n* zones within a single chip. The motivation of the present paper is that in a similar manner a stepwise change in the chemistry might create some asymmetrical wave propagation phenomena. In other words, we want to construct a chemical diode with a working principle analogous to the semiconductor device. In our experiments, waves propagate across boundaries of regions with high (H) and low (L) catalyst concentrations fixed to a polysulfone membrane. There is no gap between the H and L regions: they are in close contact. The amplitude of the waves in the membrane is controlled by the concentration of the fixed catalyst: the higher the amount of the catalyst in a region, the larger the wave amplitude there. A frequency-dependent asymmetry of the wave propagation was found: high-amplitude waves can initiate low-amplitude ones across the boundary more frequently than vice versa. Applying the concept of refractoriness,²⁵ this means

$$R(H \rightarrow L) < R(L \rightarrow H) \quad (1)$$

where $R(H \rightarrow L)$ is the recovery time (or refractoriness) of the medium L when it is perturbed by high-amplitude waves across its boundary and $R(L \rightarrow H)$ means the same when waves cross the border in the $L \rightarrow H$ direction.²⁶ To measure this asymmetry quantitatively, rotating chemical wavefronts were generated propagating in two concentric annular regions with high and

* Corresponding author. E-mail: noszti@phy.bme.hu. Fax: ++ 36-1-463-1896.

[†] Technical University of Budapest.

[‡] Institut Non Lineaire de Nice.

[§] Philipps Universität Marburg.

low amplitudes. With this construction, wave initiation phenomena can be observed periodically in both directions across the common boundary of the annuli and the two different recovery times can be determined in the asymptotic state. Finally, some interesting examples of co- and counterrotating "chemical pinwheels"^{7,12,13} are also presented.

Experimental Section

Chemicals. All chemicals applied here were of reagent grade and used without further purification: 4,7-diphenyl-1,10-phenanthroline (bathophenanthroline, Aldrich), malonic acid, sodium bromate, sodium bromide, sulfuric acid, and $(\text{NH}_4)_2\text{SO}_4$ (Fluka).

Preparation of the Catalyst-Free BZ Solution. The BZ reagent was prepared in a 500 mL stopped flask. Malonic acid (4.16 g, 0.04 mol), NaBrO_3 (6.04 g, 0.04 mol), and NaBr (3.14 g, 0.05 mol) were dissolved in 110 mL of water. Then 20 mL of 5 M sulfuric acid solution was added. When the yellow color of the bromine disappeared a solution, of 21 g (0.159 mol) of ammonium sulfate dissolved in 60 mL of water was added.

Preparation of the Catalytic Membranes. Two types of membranes were produced: (i) faintly and (ii) strongly painted membranes, with low and high catalyst concentration, respectively.

(i) A dry polysulfone membrane was placed into a solution of bathophenanthroline in glacial acetic acid (20 mg/10 mL) for 3 min, and then it was transferred to an aqueous solution ($[\text{H}_2\text{SO}_4] = 0.1 \text{ M}$, $[\text{Fe(II)}] = 0.01 \text{ M}$) for another 3 min. Finally it was washed and stored in a 0.1 M aqueous ammonium hydrogen sulfate solution.

(ii) The strongly painted membrane was prepared in a similar way but with the following differences. The bathophenanthroline concentration was higher, 250 mg/10 mL, and there was an intermediate solution with the same Fe(II) concentration but with a higher sulfuric acid concentration (0.5 M) and the membrane was kept there for only 1 min. (This solution can be used only once, all others can be applied several times.) Then the procedure continued as in (i), applying the same aqueous solution for 3 min and washing and storing the membrane in the same way.

Membranes are washed and stored in electrolyte solutions because a part of the bathoferroin would dissolve in pure water. Electrolytes strongly diminish the solubility of the catalyst.

Creating Chemical Pinwheels in Annular Membranes. A glass-fiber filter paper disk (Macherey-Nagel, MNGF-2, diameter 55 mm) was placed into a Petri dish soaked with the BZ reagent mixture, and a catalytic membrane was placed on its top. After some minutes the membrane becomes excitable and waves can be initiated in it, for example, with a silver wire. Clockwise and counterclockwise fronts are generated in pairs this way. Rotating pinwheel structures can be obtained by eliminating clockwise or counterclockwise waves by touching them with a metal paper clip.

Reactor. The reactor applied in our experiments can be seen in Figure 1. The aim of this construction was to make manipulations with the membranes as simple as possible. The 2 mm thick polyacrylamide gel disk was soaked in the BZ solution for at least 2 h before the experiments. This gel is a reservoir for the reagents, and it is big enough to run experiments for days. Before and after the experiment, the gel disk was stored in the BZ solution. The thin plastic foil pressed the membrane sandwich together to ensure a safe contact everywhere between the upper and lower membranes.

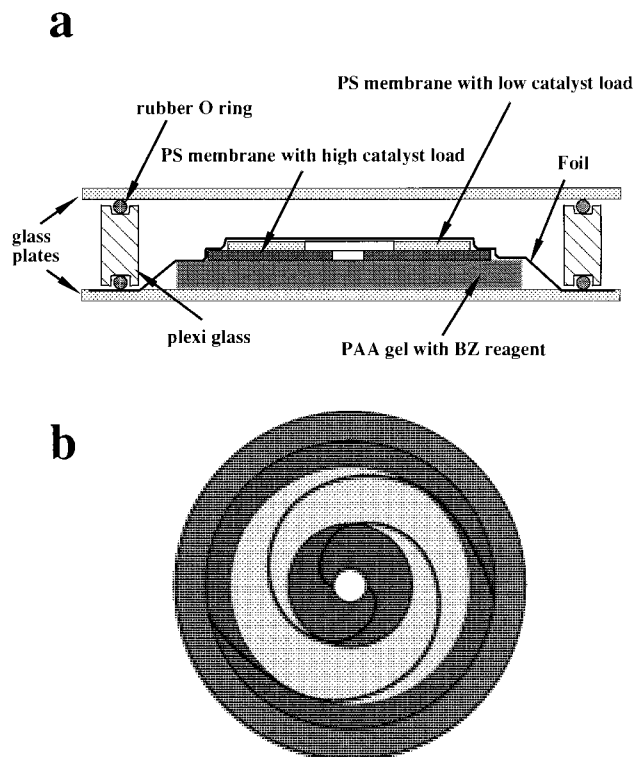


Figure 1. Arrangement of the strongly and faintly painted membranes in the first experiment: (a) cross-sectional, (b) top view.

Results and Discussion

In the experiments, so-called chemical pinwheels^{7,12,13} are applied. The advantage of such rotating structures is that the wave dynamics can be studied in an asymptotic state. This way the observations are not affected by uncertainties in the initial conditions, and the reproducibility is improved.

Demonstration of a Diode Effect with a Membrane Sandwich. In this first experiment a faintly painted membrane ring is placed on the top of a strongly painted one, and then a two-armed pinwheel is created. The experimental arrangement of this membrane sandwich is shown in Figure 1. In the asymptotic state (Figure 2a,b) the phase shift is π between the two arms, and the wavefronts in the upper and lower membrane are rotating together in a counterclockwise direction in this case. Next, a perturbation is applied: the upper membrane is lifted, turned upside down, and placed back on the top of the lower one. Now the waves in the upper, faintly painted membrane would like to travel in the opposite, that is, in clockwise, direction while waves in the lower, strongly painted membrane are still rotating in the original counterclockwise direction. Very soon, however, the upper clockwise waves are eliminated and the lower counterclockwise waves break through to the upper membrane (Figure 2c,d). Then the waves continue to rotate in both membranes together (Figure 2e,f). This series of events demonstrate certainly a diode effect: waves coming from the strongly painted membrane can initiate waves in the faintly painted one but not vice versa. At a first glance the experiment seems to suggest an unconditional unidirectional wave propagation, but this is not the case. It is true that in the above experiment low-amplitude waves failed to initiate waves in the strongly painted membrane. On the other hand, that membrane was always in an excited or in a recovery state but not in complete rest because the length of the recovery time was limited by the rotating pinwheel. Separate experiments revealed that after a long enough waiting time even a low-amplitude wave

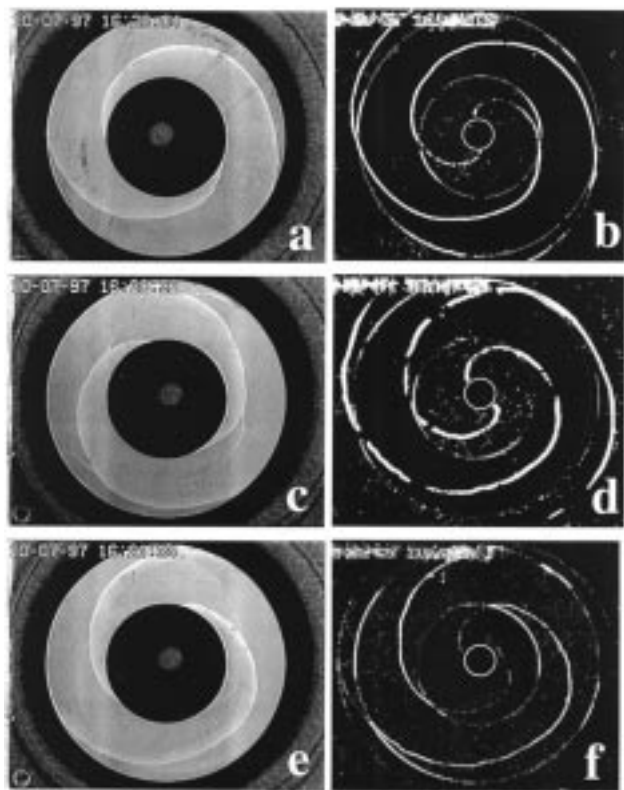


Figure 2. Unidirectional wave propagation from a strongly painted membrane to a faintly painted one. (a) A two armed pinwheel rotating counterclockwise in both membranes. (Waves in the dark membrane cannot be seen because their contrast is low.) (b) The same pinwheel subtracting two consecutive pictures to enhance the contrast of the moving fronts. (c) Waves in the faintly painted membrane after it was turned upside down. Original waves of the upper membrane are oriented in a clockwise direction now. Counterclockwise fronts from the lower membrane start to appear. (d) The same situation with picture subtraction reveals that the clockwise fronts are trapped; thus, only the more faint but living counterclockwise waves can be seen in this picture. (e) After one more minute only counterclockwise waves can be seen. (f) The same pinwheel with picture subtraction.

can initiate a high-amplitude one in the strongly painted membrane. That is, a finite recovery time denoted by $R(L \rightarrow H)$ exists, and if the following condition (eq 2) is met, then

$$R(L \rightarrow H) < \Delta t \quad (2)$$

waves can propagate not only in the $H \rightarrow L$ but in the $L \rightarrow H$ direction as well. (Here Δt is the time elapsed since the last high-amplitude wave.) In this case, the asymmetric wave propagation disappears. Also, if we study Figure 2c,d more carefully we can discover that high-amplitude waves were not able to initiate low-amplitude ones immediately where the clockwise and counterclockwise waves crossed each other. In other words, a shorter but also finite recovery time—denoted by $R(H \rightarrow L)$ —is necessary for the high-amplitude wave too before it can initiate a new wave in the wake of an old one in the faintly painted membrane. If

$$\Delta t < R(H \rightarrow L) \quad (3)$$

then no wave can cross the boundary. As can be seen, our diode has limitations because at (i) low frequencies (when eq 2 is met) all waves pass through in both directions and (ii) at high frequencies (eq 3) no second wave is able to pass through in either direction.

Thus the diode effect is not unconditional: it can be observed only for a second wave and the time separation between the waves should be in the following interval:

$$R(H \rightarrow L) < \Delta t < R(L \rightarrow H) \quad (4)$$

In this interval our diode works: second waves can propagate in the $H \rightarrow L$ direction but not in the opposite direction.

To characterize the asymmetric wave propagation quantitatively we have to determine the “cross”-recovery times²⁶ $R(H \rightarrow L)$ and $R(L \rightarrow H)$. One way to do this would be to apply a wave generator with a variable frequency. The procedure would include two separate series of experiments: one for waves penetrating from the low- to the high-amplitude medium and another for the reverse direction. In the latter case there is a limitation, however, as the waves in the high-amplitude medium cannot be started with a higher than critical frequency, determined by the self recovery time $R(H \rightarrow H)$. So the response of the low-amplitude medium to supercritical frequencies cannot be studied this way. Thus we have chosen a different approach, where both recovery times can be determined in a single experiment and no external wave source is necessary. To achieve our goal we had to create (i) an excitable membrane ring with two concentric regions for high- and low-amplitude waves and (ii) special initial conditions.

Creating Concentric Annular Zones for High- and Low-Amplitude Waves. An important requirement in our experiments is that the different zones should be in close contact with each other to obtain a reproducible wave propagation across the zone boundaries. In this respect, the best solution would be to create zones of high and low catalyst concentrations within the very same membrane. Otherwise, the experimental results might be affected by small gaps due to any imperfect fitting of two separate membranes. Small gaps can cause such problems especially when the membranes are in contact with their edges only. To paint two homogeneous zones on the very same membrane with highly different catalyst concentrations is a rather difficult task, however. Moreover, the visibility of the waves in the strongly painted membrane is very poor as Figure 2 shows. Thus we developed a different technique suggested by the sandwich experiment described in the previous paragraph. If a small piece of a strongly painted membrane is placed under a larger faintly painted one, then wave propagation in the region where they are in contact is determined by the stronger one. Thus the sandwich area behaves like a single strongly painted membrane but the upper and lower parts of the sandwich can be painted separately. This way it is easy to produce homogeneous areas with sharp boundaries, and also the visibility of the waves is good everywhere. As the contacting membrane areas are relatively large, gap problems are minimized here. It is important to note that in this construction the wave crosses the zone boundary in the upper membrane which is continuous. In our experiments we applied a strongly painted membrane ring (outer diameter 47 mm, inner diameter 20 mm) and a faintly painted membrane ring (outer diameter 40 mm, inner diameter 5 mm). The two rings were placed on a BZ-containing gel disk concentrically with the faint one on the top (Figure 3). Before putting the upper membrane on the top, however, a white, unpainted membrane disk was inserted into the hole of the lower membrane. This additional membrane was necessary to establish a uniform contact between the gel and the upper membrane. Finally the whole structure was covered with a thin plastic foil to keep the membranes together. The result of this procedure is an excitable medium with an inner and an outer annular

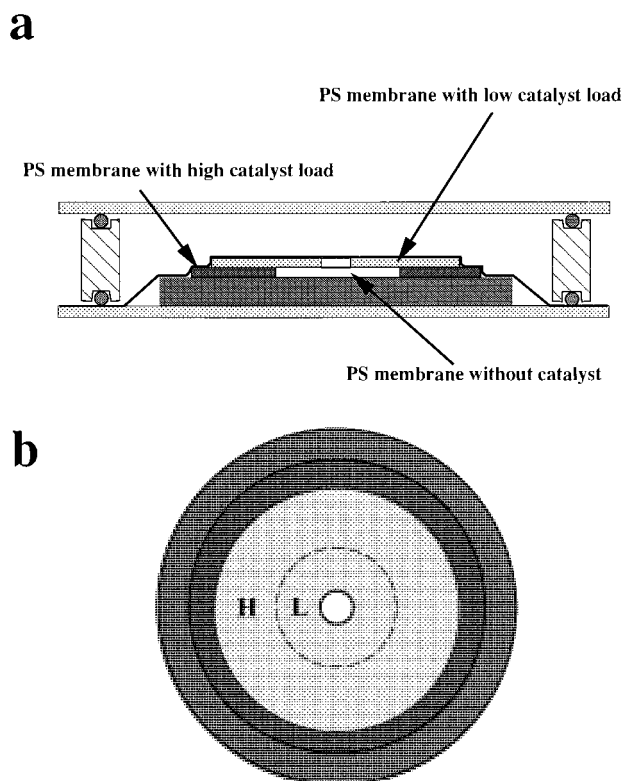


Figure 3. Sandwich structures to create zones with high and low wave amplitudes: (a) cross-sectional and (b) top view of the membrane arrangement.

region, the former for the low and the latter for the high-amplitude waves, respectively.

Generating Special Initial Conditions. The special initial conditions were rotating pinwheels but the number of the arms or/and their orientation was different in the inner and outer rings. To this end different asymptotic states (pinwheels or a uniform steady state) were established on the two membrane rings separately before they were put together into the same reactor. See, for example, Figure 4. This procedure created initial conditions with free wavefront ends. These free ends do not rotate or meander freely in the H or L regions, but they propagate strictly on the HL boundary like a reverberator.²⁵

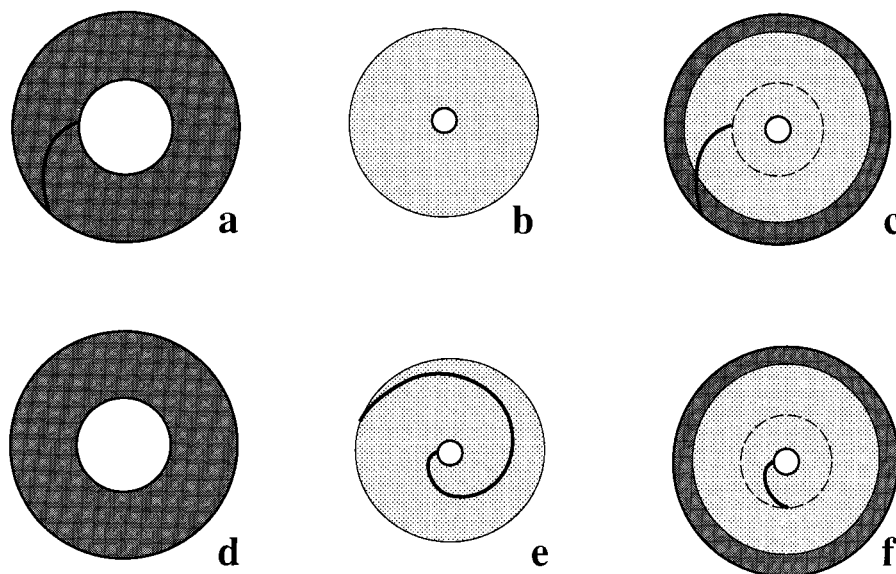


Figure 4. Initial states of the sandwich components before and just after putting them together: (a–c) initial conditions for the wave dynamics shown in Figure 5, (d–f) initial conditions for the wave dynamics shown in Figure 6.

Measurement of the Asymmetric Recovery Times. To determine the recovery times $R(L \rightarrow H)$ and $R(H \rightarrow L)$, basically the same procedure was applied. Let us consider the determination of $R(L \rightarrow H)$ as an example. As a first step we have to find the critical moment, or time of initiation $t_i(L \rightarrow H)$, when a new wavefront is initiated in the outer zone H by a low-amplitude wave of zone L. A free end, created by the special initial conditions of the previous paragraph, will act as a wave initiator. This will be illustrated with a series of snapshots shown in Figure 5. The initial condition applied for Figure 5 is depicted in Figure 4a–c. In Figure 5a, a wavefront with a free end rotates around the central hole of the membrane in region L. The free end propagates along the HL boundary, but at this stage it is not able to initiate a wave in region H because that medium is not yet recovered enough at the contact point. Zone H is recovering after the latest wave, often mentioned as “conditioning wave”,²⁷ which previously passed through the contact point. The conditioning wave can also be seen in Figure 5a. As the free end is moving along the HL boundary, it will finally arrive to a point which is recovered enough to be excited by low-amplitude waves. Then a new wavefront will be initiated in region H. This is shown in Figure 5b,c. The initiation time $t_i(L \rightarrow H)$ can be determined by looking at the development of the new front and extrapolating back to the point of origin $P_i(L \rightarrow H)$. The initiation point was marked, and stepping back in time with the recorded pictures, the time $t_c\{P_i(L \rightarrow H)\}$ when the previous wave (conditioning wave) crossed this point was determined. Then $R(L \rightarrow H)$ was calculated according to eq 5

$$R(L \rightarrow H) = t_i(L \rightarrow H) - t_c\{P_i(L \rightarrow H)\} \quad (5)$$

$R(H \rightarrow L)$ was determined by a similar procedure, applying eq 6 a formula analogous to eq 5:

$$R(H \rightarrow L) = t_i(H \rightarrow L) - t_c\{P_i(H \rightarrow L)\} \quad (6)$$

In these experiments the $H \rightarrow L$ excitation is difficult to locate (see Figure 5d). This is due to the fact that the back of the conditioning wave is close, thus the inhibitor concentration is high in the HL boundary. Consequently, the front at the free end is very faint and its position is somewhat uncertain. In a

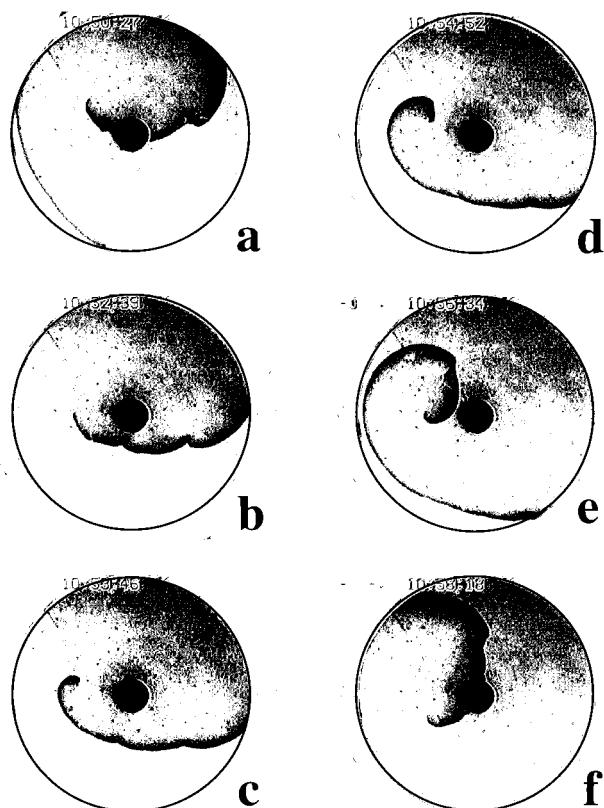


Figure 5. Cyclic evolution of the wavefronts with the initial condition shown in Figure 4a–c. (One clockwise rotating wave in the outer ring, and no waves in the inner ring.) To enhance visibility “negative” images are shown here. (The waves are black and background is white.) Snapshots a–f show some characteristic stages of the cyclic evolution in time sequence. (a) There are three wavefronts in the picture. One has a free end and rotates around the center hole counterclockwise (position: 10 o’clock). The free end propagates along the boundary of the outer (H) and the inner (L) regions. A second wavefront rotates clockwise (position: 2 o’clock). (Actually, this second and the first front together formed one single front before, but the central hole separated them.) A third wavefront (the so called conditioning wave) just leaves the reactor in the direction of 8 o’clock. (b) The first and the second front have merged again to a single front, and the third wave has left the reactor. The free end survived and just starts to initiate a new wavefront in the outer region. (c) As the new wave penetrates into the outer region now, the free end propagates in a clockwise direction along the boundary and will initiate a wave in the inner region soon. (d) A new wavefront has appeared now in the inner zone. The position of the free end is difficult to locate. (e) The free end propagates again along the boundary in a counterclockwise direction. (f) A situation somewhat similar to part a but the position of the free end points to 8 o’clock and there is no third wavefront.

later stage (Figure 4e), the free end returns to the HL boundary. On the basis of three parallel experiments with the same initial condition as in Figure 4, the following results were obtained:

$$R(L \rightarrow H) = 329 \pm 16 \text{ s}, \quad R(H \rightarrow L) = 193 \pm 20 \text{ s}, \quad \text{and} \\ A = R(L \rightarrow H)/R(H \rightarrow L) = 1.71 \pm 0.19 \quad (7)$$

where A is the measured asymmetry of the cross recovery times.

The measurements were repeated with a different initial condition (see Figure 4d–f and Figure 5). Comparing Figures 5 and 6 the only difference is the number of the clockwise rotating waves. (This number, if counterclockwise waves are counted as negative ones, is 1(H) and 0(L) for all snapshots in Figure 5 and 0(H) and 1(L) for all snapshots of Figure 6. These numbers are fixed by the initial conditions.) The results for

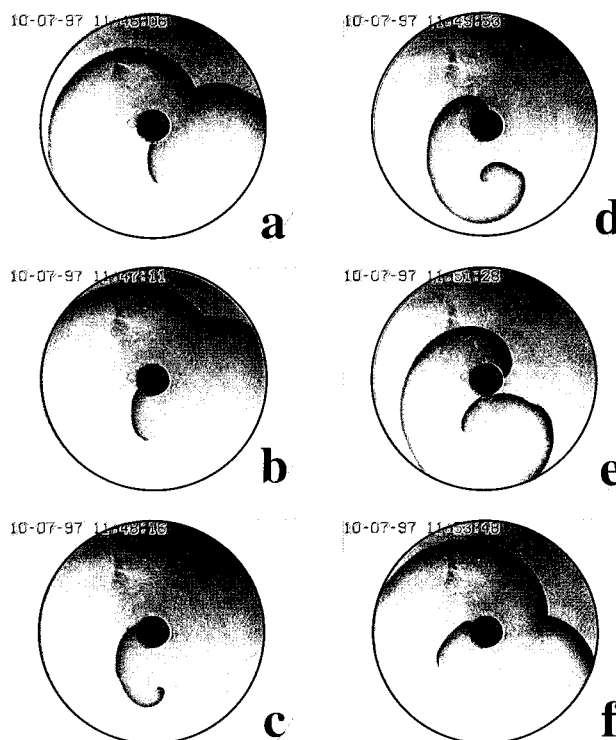


Figure 6. Cyclic evolution of the wavefronts with the initial condition shown in Figure 4d–f (one front rotating clockwise in the inner ring, and no waves in the outer ring). Negative images. (a) A wavefront with a free end rotates clockwise in the inner zone. The free end propagates along the HL boundary. The conditioning wavefront is leaving the reactor. (b) The free end initiates a front in the outer ring. (c) While this new part of the front expands, the free end propagates in a counterclockwise direction and will initiate again a wave in the inner zone. (d) The latest part of the front in the inner zone expands, and this way the free end propagates along the boundary in a clockwise direction again. (e) The wavefront hits the perimeter of the reactor and its central hole and separates into three segments this way. (f) After the merger of two wavefronts, the situation is qualitatively similar to that in part a.

the case shown in Figure 6, calculated from five parallel experiments, is

$$R(L \rightarrow H) = 284 \pm 17 \text{ s}, \quad R(H \rightarrow L) = 167 \pm 13 \text{ s}, \quad \text{and} \\ A = 1.70 \pm 0.17 \quad (8)$$

Thus, while the measured recovery times are somewhat different with the two different initial conditions, the asymmetries calculated from the data agree within the experimental error.

Coexisting Pinwheel Structures in the Inner and Outer Rings.

As Figures 5 and 6 show, the number of the pinwheel arms in the inner and outer regions is determined by the initial conditions, and these numbers are preserved in the course of the experiment. This conservation law suggested the idea that maybe more complicated pinwheel structures can coexist if an appropriate initial condition is created. In Figure 7, two of such complex structures are shown. Initial conditions for Figure 7a were a counterclockwise rotating four-armed pinwheel on the strongly painted membrane ring and a three-armed pinwheel rotating in the same direction on the faintly painted membrane. Initial conditions for Figure 7b were created by a perturbation of the structure shown in Figure 7a. The upper faintly painted membrane ring was lifted, then turned upside down, and finally placed back to the lower strongly painted membrane. These complex rotating structures were observed for several hours, and while the shape and position of the pinwheel arms were

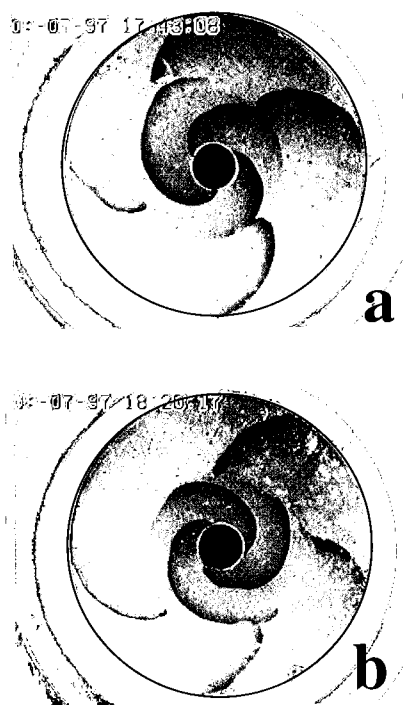


Figure 7. A four-armed pinwheel in the outer ring and a three-armed pinwheel in the inner ring. Negative images. Pinwheels rotating (a) in the same and (b) in the opposite direction.

changing continuously during these experiments, the number of arms was preserved. The relative stability of these structures is due to the greater number of arms. With many arms, both regions are mostly in the refractory state and perturbations crossing the H–L boundary have a limited effect.

Conclusion and Comments

It is known that polysulfone membranes with fixed bathoferrin catalyst can be applied advantageously to study chemical waves in a nearly 2D medium.^{12,13,18,20,22} In the present work the amount of the catalyst fixed on the membrane was varied. This way the amplitude of the waves could be controlled. It was possible to create separate H and L regions within the same membrane for the high- and low-amplitude waves, respectively. A special feature of such a system is an asymmetric wave propagation across the HL boundary: waves can propagate in the H → L direction more frequently than in the opposite way, that is, the cross-recovery time $R(H \rightarrow L)$ is shorter than $R(L \rightarrow H)$. In conclusion, we make three comments on various aspects of the asymmetric wave propagation phenomena reported here.

(i) The asymmetry can create a complex dynamical behavior for two consecutive waves (often called conditioning and test waves²⁷) following each other within a time interval which is larger than $R(H \rightarrow L)$ but smaller than $R(L \rightarrow H)$, especially in the case when region H is an isolated “island” in the “sea” of L. In this case, region H forms an obstacle for a test wave propagating in region L, but this obstacle is a temporary one only and finally the test wave may enter this area. Such an excitable medium with nonuniform recovery times (a dispersion in refractoriness) may show phenomena similar to the ones observed in some models of the cardiac muscle.^{28,29} Investigations to exploit this possibility are in progress.

(ii) The complex spatio-temporal behavior of the various pinwheel structures also deserve a comment. This complex behavior is due to the presence of at least three different

characteristic times (or frequencies). These are the rotation time(s) of the pinwheel(s) and the two different cross-recovery times. Thus a reverberator²⁵ type motion of the free ends along the HL boundary is combined with the rotation of the pinwheel(s), resulting in a complicated motion of the fronts.

(iii) Finally it is interesting to make a comparison with some recent results of Zhabotinsky and co-workers.^{17,30} They observed BZ waves propagating almost independently along the top and the bottom of a thin gel layer in the presence of an oxygen gradient perpendicular to the gel. As Figure 6 shows, we also observed a similar phenomena with rotating pinwheels. They found, however, that in their case the upper and lower excitable layers should be separated by a third, poorly excitable sublayer. In contrast there is no such poorly excitable sublayer in our experiments because a single HL boundary can separate effectively the weakly interacting rotating pinwheels shown in Figure 6.

Acknowledgment. We thank M. Wittmann, H. Farkas, and P. Simon for stimulating discussions. This work was partially supported by OTKA (T-017041) and FKFP (0287/1997) grants and by the Deutsche Forschungsgemeinschaft. Z.N. is also thankful for support by CNRS.

References and Notes

- (1) Field, R. J.; Burger, M., Eds. *Oscillations and Traveling Waves in Chemical Systems*; Wiley: New York, 1985.
- (2) Scott, S. K. *Oscillations, Waves and Chaos in Chemical Kinetics*; Oxford Univ. Press: Oxford, 1994.
- (3) Kapral, R.; Showalter, K., Eds. *Chemical Waves and Patterns*; Kluwer: Dordrecht, Netherlands, 1995.
- (4) Winfree, A. T. *When Time Breaks Down*; Princeton Univ. Press: Princeton, NJ, 1987.
- (5) Murray, J. D. *Mathematical Biology*; Springer: Berlin, 1989.
- (6) Winfree, A. T. *Science* **1994**, *266*, 1003.
- (7) Zaikin, A. N.; Zhabotinsky, A. M. *Nature* **1970**, *225*, 535.
- (8) Winfree, A. T. *Sci. Am.* **1974**, *230*, 82.
- (9) Agladze, K. I.; Krinsky, V. I. *Nature* **1982**, *296*, 424.
- (10) Winfree, A. T. In *Periodicities in Chemistry and Biology*; Eyring, H., Henderson, D., Eds.; *Progress in Theoretical Chemistry*; Academic Press: New York, 1978; Vol. 4, p 1.
- (11) Noszticzius, Z.; Horsthemke, W.; McCormick, W. D.; Swinney, H. L.; Tam, W. Y. *Nature* **1987**, *327*, 619.
- (12) Dulos, E.; Boissonade, J.; De Kepper, P. *Physica A* **1992**, *188*, 120.
- (13) Yamaguchi, T.; Kuhnert, L.; Nagy-Ungvarai, Zs.; Müller, S. C.; Hess, B., *J. Phys. Chem.* **1991**, *95*, 5831.
- (14) DeSimone, J. A.; Beil, D. L.; Scriven, L. E. *Science* **1973**, *180*, 946.
- (15) Winston, D.; Arora, M.; Maselko, J.; Gáspár, V.; Showalter, K. *Nature* **1991**, *351*, 132.
- (16) Lázár, A.; Noszticzius, Z.; Nagy-Ungvarai, Zs.; Försterling, H. D. *Physica D* **1995**, *84*, 112.
- (17) Lázár, A.; Noszticzius, Z.; Farkas, H.; Försterling, H. D. *Chaos* **1995**, *5*, 443.
- (18) Zhabotinsky, A. M.; Eager, M. D.; Epstein, I. R. *Phys. Rev. Lett.* **1993**, *71*, 1526.
- (19) Steinbock, O.; Zykov, V. S.; Müller, S. C. *Phys. Rev. E* **1993**, *48*, 3295.
- (20) Markus, M.; Stavridis, K. *Philos. Trans. R. Soc. London* **1994**, *347*, 601.
- (21) Zhabotinsky, A. M.; Györgyi, L.; Dolnik, M.; Epstein, I. R. *J. Phys. Chem.* **1994**, *98*, 7981.
- (22) Steinbock, O.; Kettunen, P.; Showalter, K. *Science* **1995**, *269*, 1857.
- (23) Oosawa, C.; Fukuta, Y.; Natsume, K.; Kometani, K. *J. Phys. Chem.* **1996**, *100*, 1043.
- (24) Lázár, A.; Försterling, H. D.; Noszticzius, Z.; Volford, A. *J. Chem. Soc., Faraday Trans.* **1996**, *92*, 2903.
- (25) Amero, J.; Lacasta, A. M.; Ramirez-Piscina, L.; Casademunt, J.; Sancho, J. M.; Sagués, F. *Phys. Rev. E* **1997**, *56*, 5405.
- (26) Lázár, A.; Försterling, H. D.; Farkas, H.; Simon, P.; Volford, A.; Noszticzius, Z. *Chaos* **1997**, *7*, 731.
- (27) Sainhas, J.; Dilao, R. *Phys. Rev. L.*, in press.
- (28) Agladze, K. I.; Aliev, R. R.; Yamaguchi, T.; Yoshikawa, K. *J. Phys. Chem.* **1996**, *100*, 13895.
- (29) Krinsky, V. I. *Biofizika* **1966**, *11*, 676.
- (30) As can be seen, the concept of recovery time was somewhat generalized here. Usually the medium is perturbed by a wave which has

the same amplitude as the wave emitted after the perturbation. These "self"-recovery times $R(L \rightarrow L)$ and $R(H \rightarrow H)$ exhibited no asymmetry in contrast with the "cross"-recovery times $R(L \rightarrow H)$ and $R(H \rightarrow L)$. It is rather probable that $R(H \rightarrow L) = R(L \rightarrow L)$. This is because $R(H \rightarrow L)$ cannot be shorter than $R(L \rightarrow L)$ otherwise waves crossing the HL boundary would not be able to propagate in L. On the other hand, regarding the high amplitude of the incoming wave, $R(H \rightarrow L)$ cannot be longer than $R(L \rightarrow L)$ either. Thus, all recovery times are roughly equal except $R(L \rightarrow H)$ which is considerably longer than the others.

(27) Gomez-Gesteria, M.; Fernandez-Garcia, G.; Munuzuri, A. P.; Perez-Munuzuri, V.; Krinsky, V. I.; Starmer, C. F.; Perez-Villar, V. *Physica D* **1994**, *76*, 359.

(28) Winfree, A. T., Ed. Fibrillation in normal ventricular myocardium. *Chaos*, **1998**, *8* (1).

(29) Xu, A.; Guevara, M. R. *Chaos* **1998**, *8*, 157.

(30) Bugrim, A. E.; Zhabotinsky, A. M.; Epstein, I. R. *J. Phys. Chem.* **1995**, *99*, 15930.